Modified Cramér-Rao bound for the estimation of the target parameters in a MIMO OFDM DFRC System

Satwika Bhogavalli, Eric Grivel, K. V. S. Hari, Vincent Corretja

Modified Cramér-Rao bound for the estimation of the target parameters in a MIMO OFDM DFRC System

Satwika BHOGAVALLI[1] Eric GRIVEL[2] K.V.S. HARI[1] Vincent CORRETJA[4]

[1]Dept. of Electrical Communication Engineering, Indian Institute of Science, Bangalore, 560012, India

[2]Bordeaux University-INP Bordeaux, IMS - UMR CNRS, 5218, France

[3]Thales Defence Mission Systems, Campus Thales Mérignac, France

Résumé – Les systèmes à double fonction radar-communication (DFRC) ont été mis en place en réponse à la pénurie spectrale en intégrant des fonctionnalités radar et de transmission reposant sur une unique forme d'onde. Tout récemment, une attention particulière a été portée à l'usage d'un système à plusieurs antennes et une forme d'onde fondée sur une approche OFDM (orthogonal frequency division multiplexing). Dans ce cas, l'un des points clés est l'estimation des paramètres des cibles tels que la direction d'arrivée (DOA), la distance et la vitesse. Dans cette communication, nous dérivons ce que l'on appelle la borne de Cramér-Rao modifiée relative à l'estimation des DOA, distances et vitesses des cibles. Puis, nous analysons de quelle manière cette borne dépend du rapport signal sur bruit et des paramètres du système tels que le nombre de sous-porteuses, de symboles OFDM et d'antennes.

Abstract – Dual-Function Radar and Communication (DFRC) systems have emerged to solve spectrum scarcity by integrating both Radar and communication functionalities based on a single waveform. Recently, a great attention has been paid to the systems based on multiple antennas and using orthogonal frequency division multiplexing (OFDM) as a waveform. In that case, one of the key issues is the estimation of the target parameters such as the direction of arrival (DOA), the range and the velocity. In this paper, we derive what is called the modified Cramér-Rao bound (MCRB) for the estimations of the DOA, range and velocity of the targets and analyze how the MCRB depends on the signal-to-noise ratio and the system parameters such as the number of sub-carriers, OFDM symbols and antennas.

1 Introduction

For the last few years, there has been a growing interest in Multiple-Input Multiple-Output (MIMO) Dual-Function Radar Communication (DFRC) systems because this system can detect targets by means of a radar and also communicate with the same hardware, by introducing transmission of information bits in a Radar waveform [5, 9, 15]. Orthogonal signals were also transmitted from multiple antennas due to the improved angular resolution [11] and the data rates. One popular waveform used in the literature for transmitting orthogonal signals from multiple antennas is the Orthogonal Frequency Division Multiplexing (OFDM). OFDM offers a high range resolution and is well-suited to combat multi-path fading.

Thus, when dealing with MIMO OFDM DFRC systems, various issues have to be addressed. One of them is the estimation of the target parameters, namely the direction of arrival (DOA), the range and the velocity. Regarding the DOA, many approaches can be used from subspace methods [6] to deep-learning based approaches [3]. In [2], we suggested estimating not only the DOA but also the range and the velocity of the targets by using subspace methods. This can be done if the Radar waveform is based on the data symbols that are replicated over a few sub-carriers and during a few OFDM symbols. As this replication can reduce the data rate in the communication part, the target ranges and velocities can be estimated by using a least-squares (LS) or total LS method. Another way to estimate the target parameters is based on the Fourier transform (FT) [13]. Its main advantage is its low computational cost. In [14], the DOAs of the different targets are jointly estimated by using a FT. Then, the estimation of the range and the velocity is based on an element-wise division between two quantities requiring the identification of the values of the main peaks of the modulus of the FT of the received signal and the term involving the DOA estimate. However, problems occur when more than one target must be detected because FT is known to be a low-resolution approach unable to discriminate the DOAs of two targets when the DOA difference is small. For this reason, in [1], we proposed an operation mode making it possible to address the estimations of the DOAs separately. Indeed, by taking advantage of the system model, the waveform can be designed so that the magnitudes of the signals back-scattered by the targets can be reduced except the one located in a specific zone. The number of zones and their limits depend on the choice of the constellation and the number of antennas. Moreover, each zone is scanned at one sub-carrier.

Another topic about DFRC systems is to optimize some performance metrics for the Radar and communication parts. Thus, in [8], the authors aim to minimize the Cramér-Rao bound (CRB) of the DOA under some constraints related to signal to interference plus noise ratio for communication users. In [12], the noise-free received-data vector is expressed as a product of two matrices: the target response matrix that depends on the DOA and a second matrix that depends on the transmitted data and the beamforming matrix. Then, the authors propose to select the antennas and then define the beamforming matrix by minimizing a criterion which is a weighted sum of the data rate and the CRB of the target response matrix.

Our work is complementary to [8, 12]. Thus, our short-term goal is to derive the CRB when dealing with the estimations of

the DOA, the range and the velocity of the targets in a MIMO OFDM DFRC system. In the system model we consider, the magnitude of the signals back-scattered by the targets are modelled by combining the Radar range equation and the Swerling model characterizing the statistical behaviour of the Radar cross section (RCS) of the target. Our purpose is to analyze the influence of the signal-to-noise ratio (SNR) and the system parameters such as the number of sub-carriers, OFDM symbols, and antennas on the CRB. Since it is not necessarily straightforward to derive the CRB due to the randomness of quantities like the RCS and the transmitted symbols, we propose to focus our attention on the modified CRB (MCRB), which was used by Gini in [4]. In our case, it consists in first considering the likelihood of the noisy observations given the RCS and the transmitted symbols, then deriving it with respect to the parameters to be estimated and finally taking the expectation with respect to the observations, the RCS and the transmitted symbols. The difference between the CRB and the MCRB is positive semidefinite [4].
The remainder of the paper is organized as follows: The system model is discussed in Section 2. The derivation of the MCRB is presented in Section 3. Finally, Section 4 provides conclusions and perspectives. In the following, * is the conjugate, $\mathbb{E}[.]$ the expectation and $\mathfrak{Re}$ the real part.

2 System Model

Let us consider a mono-static MIMO radar in a DFRC system based on a uniform linear array of L transmit antennas and $M(=L)$ receive antennas. d is the distance between two antennas. Then, an OFDM waveform is employed based on G sub-carriers with a sub-carrier spacing Δf. The data symbols are first modulated over the sub-carriers with the inverse discrete Fourier transform (IDFT). A cyclic prefix (CP) is then added and the samples are converted to an analog signal. The L transmit antennas transmit U OFDM symbols, each of duration T seconds. Given the above description, let us define $s_l(t)$ the baseband equivalent version of the transmitted signal from the l^{th} transmit antenna, with $l = 0, \cdots, L-1$ [2]:

$$s_l(t) = \sum_{u=0}^{U-1} \sum_{g=0}^{G-1} s(g,u,l) \exp\left(j2\pi g \Delta f t\right) \text{rect}\left(\frac{t-uT}{T}\right) \quad (1)$$

where $s(g,u,l)$ is the data symbol modulated over the g^{th} sub-carrier, $f_g = f_c + g\Delta f$ (with f_c the carrier frequency), during the u^{th} OFDM symbol transmitted by the l^{th} antenna. Note that as the symbols $s(g,u,l)$ are normalized for $g = 0, \cdots, G-1, u = 0, \cdots, U-1$ and $l = 0, \cdots, L-1$ and uniformly drawn from a given constellation. The set of $s(g,u,l)\ \forall\ l$ consists of i.i.d. zero-mean uniformly-distributed random variables with unit variance. This implies that:

$$\mathbb{E}[s^*(g,u,l)s(g,u,l^{'})] = \begin{cases} 1 & \text{if } l = l^{'} \\ 0 & \text{if } l \neq l^{'} \end{cases} \quad (2)$$

Assuming that there are K targets defined by their DOAs $\{\theta_k\}_{k=1,\ldots,K}$, ranges $\{D_k\}_{k=1,\ldots,K}$ and velocities $\{v_k\}_{k=1,\ldots,K}$, the ideal baseband signal $y_m(t)$, received by the m^{th} antenna can be written as follows:

$$y_m(t) = \sum_{k=1}^{K} \alpha_k \sum_{l=0}^{L-1} s_l(t-\tau_k) \exp\left(j2\pi f_k^d t\right) \quad (3)$$

where α_k is the multiplicative constant defined from the Radar range equation and the Swerling model 1. It is given by [1]:

$$\alpha_k = \frac{\lambda_c \sigma_k^{1/2}}{(4\pi)^{3/2} D_k^2} \quad (4)$$

where λ_c is the ratio between the velocity of light denoted as c and f_c. Moreover, σ_k is the RCS of the k^{th} target. Given the Swerling model 1, $\sigma_k \sim \exp(\sigma_{\text{avg}})$ with σ_{avg} the statistical mean of the target RCS. Note that $\sigma_k^{1/2}$ is a Rayleigh distributed random variable with scale parameter $\frac{1}{\sqrt{2\sigma_{\text{avg}}}}$. When more than one target is considered, the following property can be useful (where k_1 and k_2 denote the target indices):

$$\mathbb{E}[(\sigma_{k_1}^*)^{1/2}\sigma_{k_2}^{1/2}] = \begin{cases} \mathbb{E}[|\sigma_{k_1}|] = \mathbb{E}[\sigma_{k_1}] = \frac{1}{\sigma_{\text{avg}}} \text{ for } k_1 = k_2 \\ \mathbb{E}[(\sigma_{k_1}^*)^{1/2}]\,\mathbb{E}[\sigma_{k_2}^{1/2}] = \frac{\pi}{4\sigma_{\text{avg}}} \text{ for } k_1 \neq k_2 \end{cases} \quad (5)$$

In addition, the delay τ_k can be approximated by:

$$\tau_k \approx 2\frac{D_k}{c} + (l+m)d\sin\theta_k \quad (6)$$

and the Doppler frequency satisfies $f_k^d \approx 2\frac{v_k f_c}{c}$.
At the receiver, after applying the DFT to the ideal received signal after converting the signal from the analog to the discrete domain and removing the CP, the received data symbols are assumed to be given by:

$$y(g,u,m) = \mu(g,u,m) + \eta(g,u,m) \quad (7)$$

where $\{\eta(g,u,m)\}_{g=0,\cdots G-1;u=0,\cdots,U-1;m=0,\cdots,M-1}$ is a set of independent and identically distributed (i.i.d.) Gaussian random variables with zero-mean and variance σ_η^2. No clutter is considered in this study. Moreover, the noise-free received signal $\mu(g,u,m)$ is given by:

$$\mu(g,u,m) = \sum_{k=1}^{K} \Gamma_k(g,u,m) \quad (8)$$

where $\Gamma_k(g,u,m)$ is the received back-scattered signal by the k^{th} target and is given by:

$$\Gamma_k(g,u,m) = \alpha_k \left[\sum_{l=0}^{L-1} s(g,u,l) \exp\left(-jl\omega_{\theta_{k,g}}\right)\right] \times \exp\left(-jm\omega_{\theta_{k,g}}\right) \exp\left(-jg\omega_{D_k}\right) \exp(ju\omega_{v_k}) \quad (9)$$

with:

$$\begin{cases} \omega_{\theta_{k,g}} = 2\pi d \sin\theta_k \frac{(f_c+g\Delta f)}{c} \\ \omega_{D_k} = \frac{4\pi\Delta f D_k}{c} \\ \omega_{v_k} = \frac{4\pi T v_k}{\lambda_c} \end{cases} \quad (10)$$

At the receiver, the signal-to-noise ratio related to the k^{th} target is defined by:

$$\text{SNR}_k = \frac{\sum_{g=0}^{G-1}\sum_{u=0}^{U-1}\sum_{m=0}^{M-1} \mathbb{E}\left[\Gamma_k(g,u,m)\Gamma_k^*(g,u,m)\right]}{\sum_{g=0}^{G-1}\sum_{u=0}^{U-1}\sum_{m=0}^{M-1} \mathbb{E}\left[\eta(g,u,m)\eta^*(g,u,m)\right]} \quad (11)$$

$$= \frac{\lambda_c^2}{64\pi^3 D_k^4 \sigma_{\text{avg}} \sigma_\eta^2} M \quad (12)$$

In the next section, we derive the MCRB for the above-mentioned system model for the single-target case for simplicity in mathematical development. Note that the same methodology can be applied when there are more targets.

1. The signal back-scattered by each target at the frequency $f_c + g\Delta f$ should be multiplied by $\alpha_{k,g} = \frac{c\sigma_k^{1/2}}{(4\pi)^{3/2}(f_c+g\Delta f)D_k^2}$. By approximating $f_c + g\Delta f$ by f_c, $\alpha_{k,0} \approx \alpha_{k,1} \cdots \approx \alpha_{k,G-1} = \alpha_k$

3 Derivation of the modified Cramér-Rao bound

The MCRB matrix $\boldsymbol{\mathcal{C}}$ is related to the modified Fisher information matrix (MFIM), $\boldsymbol{\mathcal{F}}$ as $\boldsymbol{\mathcal{C}} = \boldsymbol{\mathcal{F}^{-1}}$. In the single-target case, the parameter vector is given by $\boldsymbol{\zeta} = \begin{bmatrix}\theta_1 & D_1 & v_1\end{bmatrix}^T$ and one has:

$$\boldsymbol{\mathcal{C}} = \begin{bmatrix} \mathcal{C}_{\boldsymbol{\theta\theta}} & \mathcal{C}_{\boldsymbol{\theta}\mathbf{D}} & \mathcal{C}_{\boldsymbol{\theta}\mathbf{v}} \\ \mathcal{C}_{\mathbf{D}\boldsymbol{\theta}} & \mathcal{C}_{\mathbf{DD}} & \mathcal{C}_{\mathbf{Dv}} \\ \mathcal{C}_{\mathbf{v}\boldsymbol{\theta}} & \mathcal{C}_{\mathbf{vD}} & \mathcal{C}_{\mathbf{vv}} \end{bmatrix} = \boldsymbol{\mathcal{F}}^{-1} = \begin{bmatrix} \mathcal{F}_{\boldsymbol{\theta\theta}} & \mathcal{F}_{\boldsymbol{\theta}\mathbf{D}} & \mathcal{F}_{\boldsymbol{\theta}\mathbf{v}} \\ \mathcal{F}_{\mathbf{D}\boldsymbol{\theta}} & \mathcal{F}_{\mathbf{DD}} & \mathcal{F}_{\mathbf{Dv}} \\ \mathcal{F}_{\mathbf{v}\boldsymbol{\theta}} & \mathcal{F}_{\mathbf{vD}} & \mathcal{F}_{\mathbf{vv}} \end{bmatrix}^{-1} \tag{13}$$

$\boldsymbol{\mathcal{F}}$ is a Hermitian matrix and can be calculated as [4] [7]:

$$\boldsymbol{\mathcal{F}} = -\mathbb{E}_{\mathbf{y},\mathbf{s},\boldsymbol{\sigma}}\left(\frac{\partial^2 \ln p(\mathbf{y}|\mathbf{s},\boldsymbol{\sigma};\boldsymbol{\zeta}}{}\partial\boldsymbol{\zeta}\partial\boldsymbol{\zeta}^T\right) \tag{14}$$

where $\mathbf{y}$ and $\mathbf{s}$ are the column vectors that stack the received and the transmitted data along the spatial, frequency and time domains respectively. The vector $\boldsymbol{\sigma}$ consists of $\{\sigma_k^{1/2}\}_{k=1}^K$. In addition, $p(\mathbf{y}|\mathbf{s},\boldsymbol{\sigma};\boldsymbol{\zeta})$ is the likelihood function of the vector $\mathbf{y}$ given $\mathbf{s}$ and $\boldsymbol{\sigma}$. The (p^{th}, q^{th}) element of $\boldsymbol{\mathcal{F}}$ is calculated based on the assumption that $p(\mathbf{y}|\mathbf{s},\boldsymbol{\sigma};\boldsymbol{\zeta})$ is a multivariate Gaussian distribution. It is given by:

$$\boldsymbol{\mathcal{F}}_{p,q} = \frac{2}{\sigma_\eta^2}\sum_{g=0}^{G-1}\sum_{u=0}^{U-1}\sum_{m=0}^{M-1}\mathfrak{Re}\left[\mathbb{E}_{\mathbf{s},\boldsymbol{\sigma}}\left[\frac{\partial\mu^*(g,u,m)}{\partial\zeta_p}\frac{\partial\mu(g,u,m)}{\partial\zeta_q}\right]\right] \tag{15}$$

where ζ_p and ζ_q are p^{th} and q^{th} elements of $\boldsymbol{\zeta}$.
In the following, we give some details to deduce the expression of $\mathcal{F}_{1,2} = \mathcal{F}_{\theta\mathbf{D}}$ as an example. Then, the other elements of the matrix are presented in a table. Finally, the analytical expression of the diagonal elements of the MCRB are given.

3.1 Expression for the element $\mathcal{F}_{\boldsymbol{\theta}\mathbf{D}}$

The expression of $\mathcal{F}_{\boldsymbol{\theta}\mathbf{D}}$ can be deduced from:

$$\mathcal{F}_{\boldsymbol{\theta}\mathbf{D}} \overset{(15)}{=} \frac{2}{\sigma_\eta^2}\sum_{g=0}^{G-1}\sum_{u=0}^{U-1}\sum_{m=0}^{M-1}\mathfrak{Re}\left[\mathbb{E}_{\mathbf{s},\boldsymbol{\sigma}}\left[\frac{\partial\mu^*(g,u,m)}{\partial\theta_1}\frac{\partial\mu(g,u,m)}{\partial D_1}\right]\right] \tag{16}$$

Using (4), (8) and (9), let us calculate $\frac{\partial\mu(g,u,m)}{\partial\theta_1}$ as follows:

$$\frac{\partial\mu(g,u,m)}{\partial\theta_1} = \frac{\lambda_c\sigma_1^{1/2}}{(4\pi)^{3/2}D_1^2}\exp\left(-jg\omega_{D_1}\right)\exp(ju\omega_{v_1}) \tag{17}$$
$$\times\left[\sum_{l=0}^{L-1}s(g,u,l)\left(-j(l+m)\frac{\partial\omega_{\theta_{1,g}}}{\partial\theta_1}\right)\exp\left(-j(l+m)\omega_{\theta_{1,g}}\right)\right]$$

with $\frac{\partial\omega_{\theta_{1,g}}}{\partial\theta_1} = 2\pi d\cos\theta_1\frac{(f_c+g\Delta f)}{c}$.
Similarly, keeping in mind that α_1 depends on D_1, $\frac{\partial\mu(g,u,m)}{\partial D_1}$ leads as:

$$\frac{\partial\mu(g,u,m)}{\partial D_1} = \frac{\lambda_c\sigma_1^{1/2}}{(4\pi)^{3/2}D_1^2}\left(-\frac{2}{D_1} - jg\frac{\partial\omega_{D_1}}{\partial D_1}\right) \tag{18}$$
$$\times\exp\left(-jg\omega_{D_1}\right)\exp(ju\omega_{v_1})\left[\sum_{l=0}^{L-1}s(g,u,l)\exp\left(-j(l+m)\omega_{\theta_{1,g}}\right)\right]$$

with $\frac{\partial\omega_{D_1}}{\partial D_1} = \frac{4\pi\Delta f}{c}$.
As $\mathbf{s}$ and $\boldsymbol{\sigma}$ are independent of each other, the expectation

Elements of $\mathcal{F}$	Expressions
$\mathcal{F}_{\boldsymbol{\theta\theta}}$	$\gamma\frac{d^2\cos^2\theta_1}{6}(7M-5)(M-1)$ $\times\left[1+\frac{\Delta f}{f_c}(G-1)+\left(\frac{\Delta f}{f_c}\right)^2\frac{(G-1)(2G-1)}{6}\right]$
$\mathcal{F}_{\boldsymbol{\theta}\mathbf{D}}$	$\gamma\frac{d\Delta f\cos\theta_1}{f_c}(G-1)(M-1)\left[1+\frac{\Delta f}{f_c}\frac{(2G-1)}{3}\right]$
$\mathcal{F}_{\boldsymbol{\theta}\mathbf{v}}$	$-\gamma Td\cos\theta_1(U-1)(M-1)\left[1+\frac{(G-1)}{2}\frac{\Delta f}{f_c}\right]$
$\mathcal{F}_{\mathbf{DD}}$	$\gamma\frac{\lambda_c^2}{\pi^2}\left[\frac{1}{D_1^2}+\frac{2\pi^2(G-1)(2G-1)(\Delta f)^2}{3c^2}\right]$
$\mathcal{F}_{\mathbf{Dv}}$	$-\gamma\frac{T\Delta f}{f_c}(G-1)(U-1)$
$\mathcal{F}_{\mathbf{vv}}$	$\gamma\frac{2T^2}{3}(U-1)(2U-1)$

Table 1 – Elements in the sub-matrices of $\mathcal{F}$

$\mathbb{E}_{\mathbf{s},\boldsymbol{\sigma}}\left[\frac{\partial\mu^*(g,u,m)}{\partial\theta_1}\frac{\partial\mu(g,u,m)}{\partial D_1}\right]$ using (2) leads to:

$$\mathbb{E}_{\mathbf{s},\boldsymbol{\sigma}}\left[\frac{\partial\mu^*(g,u,m)}{\partial\theta_1}\frac{\partial\mu(g,u,m)}{\partial D_1}\right] = -\frac{\lambda_c^2\,\mathbb{E}[\sigma_1]}{(4\pi)^3D_1^4}\frac{\partial\omega_{\theta_{1,g}}}{\partial\theta_1} \tag{19}$$
$$\times\left(\frac{2j}{D_1} - g\frac{\partial\omega_{D_1}}{\partial D_1}\right)\left[\sum_{l=0}^{L-1}(l+m)\right]$$

Since $\mathbb{E}[\sigma_1] = \frac{1}{\sigma_{\text{avg}}}$ and after further simplification, one gets:

$$\mathcal{F}_{\boldsymbol{\theta}\mathbf{D}} = \frac{d\Delta f\cos\theta_1\gamma}{f_c}(G-1)(M-1)\left[1+\frac{\Delta f}{f_c}\frac{(2G-1)}{3}\right] \tag{20}$$

where $\gamma = \frac{GUM^2}{8\pi\sigma_\eta^2\sigma_{\text{avg}}D_1^4}$.
Following a similar procedure, all the elements in $\mathcal{F}$ can be calculated and are presented in Table (1).
Then, the MCRB matrix can be deduced by inverting the MFIM. In the next sub-section, we focus our attention on the diagonal elements of the MCRB matrix for the sake of space.

3.2 Diagonal elements of the MCRB matrix

From the 3×3 matrix $\boldsymbol{\mathcal{F}}$, the analytical expression of each diagonal element of the MCRB matrix can be expressed as the ratio of polynomials in $\frac{\Delta f}{f_c}$. Thus, one gets:

$$\mathcal{C}_{\boldsymbol{\theta\theta}} = \beta\frac{\beta_{0,n}+\beta_{2,n}(\frac{\Delta f}{f_c})^2}{\beta_{0,d}+\beta_{1,d}\frac{\Delta f}{f_c}+\beta_{2,d}\left(\frac{\Delta f}{f_c}\right)^2} \tag{21}$$

where β, $\beta_{0,n}$, $\beta_{2,n}$ and $\{\beta_{q,d}\}_{q=0,1,2}$ [2] are weights depending on products of quantities such as $G-1$, $2G-1$, $7G-5$, $U-1$, $2U-1$, $M-1$, but also D_1, d, SNR_1, etc. It leads to expressions that are too long to be presented in this communication. Therefore, we suggest making a few approximations [3] such as $G-1\approx G$, $(U-1)\approx U$ and $M-1\approx M$ to provide an approximation of the diagonal terms of $\boldsymbol{\mathcal{C}}$, *i.e.* $\hat{\mathcal{C}}_{\boldsymbol{\theta\theta}}, \hat{\mathcal{C}}_{\boldsymbol{DD}}$ and $\hat{\mathcal{C}}_{\boldsymbol{vv}}$. In that case, one gets:

$$\beta \approx \frac{1}{8\pi^2d^2\cos^2\theta_1 GUM^3\text{SNR}_1} \tag{22}$$

2. The index n refers to the numerator while d refers to the denominator.
3. G, U and M are assumed to between ten to a few tens, but larger values could also be considered.

and:

$$\begin{cases} \beta_{0,n} \approx \frac{4}{3}\frac{\lambda_c^2}{\pi^2 D_1^2} \text{ and } \beta_{2,n} \approx \frac{7}{9}G^2 \\ \beta_{0,d} \approx \frac{5}{9}\frac{1}{\pi^2 D_1^2} + \frac{13}{54}\frac{G^2(\Delta f)^2}{c^2} \\ \beta_{1,d} \approx \frac{5}{9}\frac{G}{\pi^2 D_1^2} + \frac{7}{54}\frac{G^3(\Delta f)^2}{c^2} \\ \beta_{2,d} \approx \frac{29}{108}\frac{G^2}{\pi^2 D_1^2} + \frac{7}{162}\frac{G^4(\Delta f)^2}{c^2} \end{cases} \tag{23}$$

Similarly, $\hat{\mathcal{C}}_{DD}$ and $\hat{\mathcal{C}}_{vv}$ can be obtained as follows [4]:

$$\hat{\mathcal{C}}_{\mathbf{DD}} = \tilde{\beta}\frac{\tilde{\beta}_{0,n} + \tilde{\beta}_{1,n}\left(\frac{\Delta f}{f_c}\right) + \tilde{\beta}_{2,n}\left(\frac{\Delta f}{f_c}\right)^2}{\beta_{0,d} + \beta_{1,d}\left(\frac{\Delta f}{f_c}\right) + \beta_{2,d}\left(\frac{\Delta f}{f_c}\right)^2} \tag{24}$$

with:

$$\tilde{\beta} \approx \frac{1}{8\pi^2 GUM\text{SNR}_1} \tag{25}$$

and:

$$\begin{cases} \tilde{\beta}_{0,n} \approx \frac{5}{9} \\ \tilde{\beta}_{1,n} \approx \frac{5}{9}G \text{ and } \tilde{\beta}_{2,n} \approx \frac{29}{108}G^2 \end{cases} \tag{26}$$

$$\hat{\mathcal{C}}_{vv} = \beta' \frac{\sum_{q=0}^{4} \beta'_{q,n}\left(\frac{\Delta f}{f_c}\right)^q}{\beta_{0,d} + \beta_{1,d}\left(\frac{\Delta f}{f_c}\right) + \beta_{2,d}\left(\frac{\Delta f}{f_c}\right)^2} \tag{27}$$

with:

$$\beta' \approx \frac{1}{8\pi^2 T^2 GU^3 M\text{SNR}_1} \tag{28}$$

and:

$$\begin{cases} \beta'_{0,n} \approx \frac{7\lambda_c^2}{6\pi^2 D_1^2} \text{ and } \beta'_{1,n} \approx \frac{7\lambda_c^2 G}{6\pi^2 D_1^2} \\ \beta'_{2,n} \approx \frac{5}{9}G^2 + \frac{7\lambda_c^2}{18\pi^2 D_1^2}G^2 \text{ and } \beta'_{3,n} \approx \frac{2}{9}G^3 \\ \beta'_{4,n} \approx \frac{2}{27}G^4 \end{cases} \tag{29}$$

First of all, the simulations we conducted confirm that the approximations are relevant. Given (21), (24) and (27), we can notice that $\hat{\mathcal{C}}_{\theta\theta}$, $\hat{\mathcal{C}}_{DD}$ and $\hat{\mathcal{C}}_{vv}$ are inversely proportional to SNR_1. In addition, we checked by simulations that $\hat{\mathcal{C}}_{\theta\theta}$ and $\hat{\mathcal{C}}_{vv}$ are inversely proportional to M^3 [10] and U^3 respectively. Moreover, from equation (21), as $\mathcal{C}_{\boldsymbol{\theta\theta}}$ depends on the inverse of $\cos\theta_1$, it increases when θ_1 tends to $\pm\frac{\pi}{2}$.
Figure 1 shows that depending on the target range, the dependency of $\hat{\mathcal{C}}_{DD}$ with G varies. Indeed, by neglecting the smallest terms in the denominator of (24), $\hat{\mathcal{C}}_{DD}$ is inversely proportional to G for smaller values of D_1 and G, whereas $\hat{\mathcal{C}}_{DD}$ is inversely proportional to G^3 for higher values of D_1.

4 Conclusions and perspectives

In a MIMO OFDM DFRC system, estimating the DOA but also the range and the velocity can be of real interest. In this communication, our purpose was to derive the MCRB in a single-target case with a few approximations in order to see how the MCRB may vary with respect to the SNR and the system parameters like the number of sub-carriers, OFDM symbols and antennas. The next step is to analyse the cross-dependency between the target parameters and to extend our study to more than one target. Finally, the derivation of the MCRB will serve as a basis to select antennas and sub-carriers in order to optimize the performance of DFRC systems in terms of data rate and accuracy of DOA, range and velocity.

4. The denominators of $\hat{\mathcal{C}}_{\theta\theta}$, $\hat{\mathcal{C}}_{DD}$ and $\hat{\mathcal{C}}_{vv}$ defined by $\{\beta_{q,d}\}_{q=0,1,2}$ are the same and are obtained from the determinant of $\boldsymbol{\mathcal{F}}$.

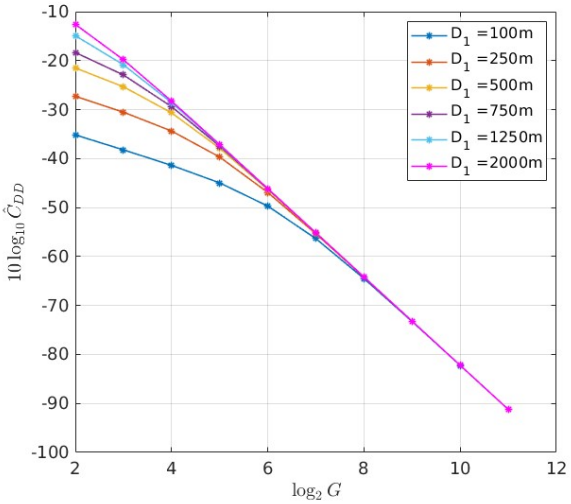

Figure 1 – Variation of $\hat{\mathcal{C}}_{DD}$ with G for different values of D_1 at $\text{SNR}_1 = 20$ dB, $U = 64$, $M = 16$, $\Delta f = 20$KHz, $f_c = 2$GHz, $(\theta_1, v_1) = (39.32^o, 31.72m/s)$

References

[1] S. Bhogavalli, E. Grivel, K.V.S. Hari, and V. Corretja. Waveform design to improve the estimation of target parameters using the fourier transform method in a MIMO OFDM DFRC system. In *IEEE ICASSP 2023*, pages 1–5, 2023.

[2] S. Bhogavalli, K.V.S. Hari, E. Grivel, and V. Corretja. Estimating the target DOA, range and velocity using subspace methods in a MIMO OFDM DFRC system. *Signal Processing*, 209:109007, 2023.

[3] J. Fuchs, M. Gardill, M. Lübke, A. Dubey, and F. Lurz. A machine learning perspective on automotive radar direction of arrival estimation. *IEEE Access*, 10:6775–6797, 2022.

[4] F. Gini, R. Reggiannini, and U. Mengali. The modified cramer-rao bound in vector parameter estimation. *IEEE Transactions on Communications*, 46(1):52–60, 1998.

[5] A. Hassanien, M. G. Amin, E. Aboutanios, and B. Himed. Dual-function radar communication systems: A solution to the spectrum congestion problem. *IEEE Signal Processing Magazine*, 36(5):115–126, 2019.

[6] A.G. Jaffer. Maximum likelihood direction finding of stochastic sources: a separable solution. In *ICASSP-88., International Conference on Acoustics, Speech, and Signal Processing*, pages 2893–2896 vol.5, 1988.

[7] S. M Kay. *Fundamentals of statistical signal processing: estimation theory*. Prentice-Hall, Inc., 1993.

[8] F Liu, Y. Liu, A. Li, C. Masouros, and Y. C. Eldar. Cramér-rao bound optimization for joint radar-communication beamforming. *IEEE Transactions on Signal Processing*, 70:240–253, 2022.

[9] S. Mercier, S. Bidon, D. Roque, and C. Enderli. Comparison of correlation-based OFDM radar receivers. *IEEE Transactions on Aerospace and Electronic Systems*, 56(6):4796–4813, 2020.

[10] P. Stoica and A. Nehorai. Music, maximum likelihood and cramer-rao bound. In *IEEE ICASSP 88*, pages 2296–2299 vol.4, 1988.

[11] S. Sun, A. P. Petropulu, and H. V. Poor. Mimo radar for advanced driver-assistance systems and autonomous driving: Advantages and challenges. *IEEE Signal Processing Magazine*, 37(4):98–117, 2020.

[12] Z. Xu, F. Liu, and A. Petropulu. Cramér-rao bound and antenna selection optimization for dual radar-communication design. In *IEEE ICASSP 2022*, pages 5168–5172, 2022.

[13] Z. Xu and A. Petropulu. A bandwidth efficient dual-function radar communication system based on a MIMO radar using OFDM waveforms. *IEEE Transactions on Signal Processing*, 71:401–416, 2023.

[14] Z. Xu, A. Petropulu, and S. Sun. A joint design of mimo-ofdm dual-function radar communication system using generalized spatial modulation. In *IEEE RadarConf 20*, pages 1–6, 2020.

[15] J. A. Zhang, F. Liu, C. Masouros, R. W. Heath, Z. Feng, L. Zheng, and A. Petropulu. An overview of signal processing techniques for joint communication and radar sensing. *IEEE Journal of Selected Topics in Signal Processing*, 15(6):1295–1315, 2021.